

# Data-driven Approach for Automatically Correcting Faulty Road Maps

Soojung Hong\*  
ETH Zürich

Department of Computer Science  
hong.soojung@gmail.com

Kwanghee Choi\*  
Sogang University

Department of Computer Science and Engineering  
juice500@sogang.ac.kr

## Abstract

Maintaining road networks is labor-intensive, especially in actively developing countries where the road frequently changes. Many automatic road extraction approaches have been introduced to solve this real-world problem, fueled by the abundance of large-scale high-resolution satellite imagery and advances in data-driven vision technology. However, their performance is limited to fully automating road map extraction in real-world services. Hence, many services employ the human-in-the-loop approaches on the extracted road maps: semi-automatic detection and repairment of faulty road maps. Our paper exclusively focuses on the latter, introducing a novel data-driven approach for fixing road maps. We incorporate image inpainting approaches to tackle complex road geometries without custom-made algorithms for each road shape, yielding a method that is readily applicable to any road map segmentation model. We compare our method with the baselines on various road geometries, such as straight and curvy roads, T-junctions, and intersections, to demonstrate the effectiveness of our approach.

## 1. Introduction

Developing and maintaining accurate road maps is essential for many applications, notably location-based services [4] and autonomous driving [35]. However, keeping the road maps up-to-date is an arduous process that often requires extensive manual labor [27, 36], spending millions and billions of dollars [16, 17]. For example, road maps are frequently changed for developing countries, where their increase in the total road length is substantial [5, 27, 55]. Further, there are more scenarios on road map updates apart from new construction of roads, such as removal or topology changes [5].

To tackle the aforementioned problem, recent advances have been dominated by utilizing aerial and satellite im-

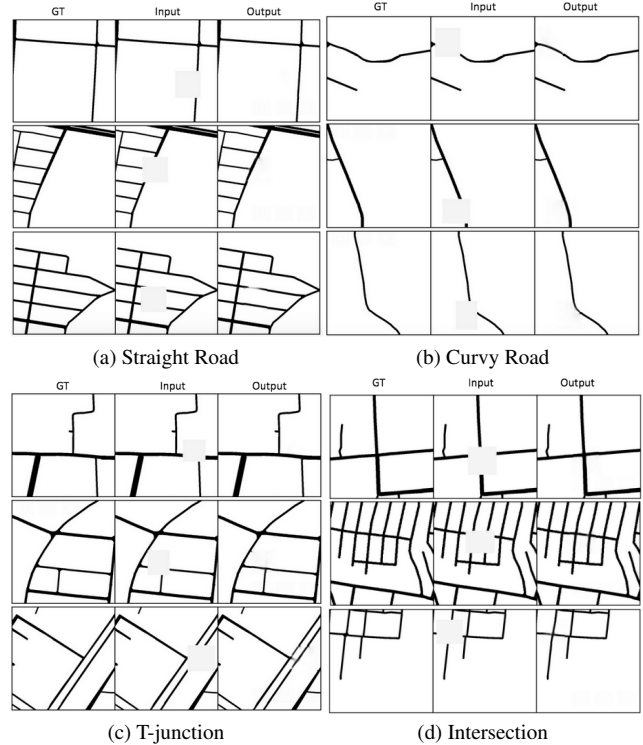


Figure 1. Road inpainting results of our method on real-world complex road types. GT, Input, and Output denotes the ground truth, the input image that the model receives, and the model prediction outputs. Our method successfully reconstructs the hidden road by capturing the geometric information of the surroundings.

agery to construct road maps [5, 30] that offer abundant, reliable, high-resolution, and real-time data [4, 30, 35, 55]. Its properties are ideal for deep learning-based vision approaches, where they are able to yield higher-quality automated road extraction at the expense of more data and computing power. Hence, with the successes of deep neural networks (DNNs), many DNN-based approaches have been introduced [30]. Notably, most state-of-the-art methods view the road extraction problem as the semantic segmentation problem [13], *e.g.*, given the aerial image, predict

\*Equal contribution.

the binary map that denotes roads as one and others as zero.

To further enhance the final performance of the segmentation model, post-processing methods are often applied [31, 41, 46, 48]. While delegating the extraction of the overall geometry of roads based on the satellite imagery to the segmentation models, post-processing methods concentrate on the finer details: restoring the missing connections between roads, removing noisy predictions, and generating final binary maps from real-valued predictions. However, in many cases, heuristics are often too simple to tackle real-world road structures with complex geometry. Real-world road geometries are not only straight or smoothly curved but too complex, often hard to categorize into a few geometric primitives [15]. Figure 2 demonstrates road geometries that are challenging to handle with unstructured complex road shapes compared to simple road primitives [15].

To tackle the limitations above, human-in-the-loop approaches are often used in industry-level applications, making the manual labor of labeling road maps much more efficient via automation. A two-step approach is commonly employed to maintain existing road maps: error localization and automatic mending [2]. Error localization recommends locations to be fixed to the labeling force, where automatic mending tries to mend the road maps without human intervention, giving a good prior for the human annotators to fix further if necessary. Automatic mending aims to fix the location by considering the neighboring road geometries, providing a good baseline for the annotators, similar to error localization. The two-step approach enables the intervention from human annotators by design, yielding an effective human-in-the-loop system.

We focus on the latter of the two-step system, the automatic mending step, to introduce a novel data-driven method that leverages the abundant amount of satellite imagery available. We borrow the image inpainting techniques [19, 40, 53, 54] regarding a faulty map region to be an area to be inpainted. Our method is easily applicable to many existing approaches as it does not require bells and whistles and is intuitive to use. Further, unlike hand-crafted heuristics, our method improves its predictive performance as data size increases. Even if a new road structure emerges, our method can cover it without any modifications if one has enough data to train, which is ideal for production use. To demonstrate the effectiveness of our approach on various road geometries, we separately evaluate on complex structures such as curvy roads, T-junctions, and intersections, where existing heuristic methods are known to fail. Our experiments confirm our approach’s superiority, qualitatively and quantitatively, without the need for heavy customization.

To summarize, our contribution is twofold: (1) introduce a novel data-driven approach for mending faulty road maps based on image inpainting techniques, and (2) demonstrate that our approach is superior via extensive evaluation with

various road geometries.

## 2. Related Works

### 2.1. Automatic Road Map Extraction

Creating road maps is a laborious process; annotators often look at overhead views of the cities to draw the roads one by one, being more and more problematic at scale [28]. On the other hand, crowd-sourced efforts such as OpenStreetMaps [39] provide scalability, even though they often suffer low resolution and misalignment, often being not reliable enough for production use [28]. To mitigate the problem, automatic road detection is often utilized, where it has been studied for more than 30 years [3]. However, finding a reliable methodology for extracting the correct road information from aerial imagery has been challenging due to the inherent nature of the road environment. The road aerial images contain a wide variety of road geometries and non-road objects such as vegetation, occlusions, and shadows along with roads [33, 38]. With the abundance of high-resolution satellite and aerial imagery, deep learning-based approaches for the automated extraction of road maps became dominant. Especially, recent approaches often regard the road extraction problem as the semantic segmentation task, i.e., pixel-wise classification of road and non-road pixel locations [4, 30]. Many strategies for training the segmentation model have been proposed, such as fully supervised [31], adversarial [44], weakly supervised [51], and unsupervised [47] approaches. Consult [30, 57] for a more comprehensive survey.

Although deep-learning-based segmentation models significantly advanced the state-of-the-art, their performance becomes unsatisfactory when roads become more complex with various types of roads mixed [1]. In particular, segmentation models based on FCN (Fully Convolutional Networks) [26, 32] empirically fail to capture the overall geometry of roads, lacking spatial consistency and road connectivity [1]. Hence, we are further motivated to attach a human-in-the-loop system to resolve the limitations of existing models [2]: components that can handle real-world complexities.

### 2.2. Post-processing Road Maps

Algorithm-driven post-processing efforts to fix incomplete road maps often concentrate on refining the quality of extracted roads. To reduce the noise of segmentation prediction outputs, state-of-the-art segmentation models often attach heuristics that are tailored toward each specific model. The morphological operation technique is used in a post-processing step when road extraction models detect road geometries [41, 45, 46, 48]. However, the morphological operation technique mainly removes non-road objects, such as vehicles or trees. Therefore, it does not improve the qual-

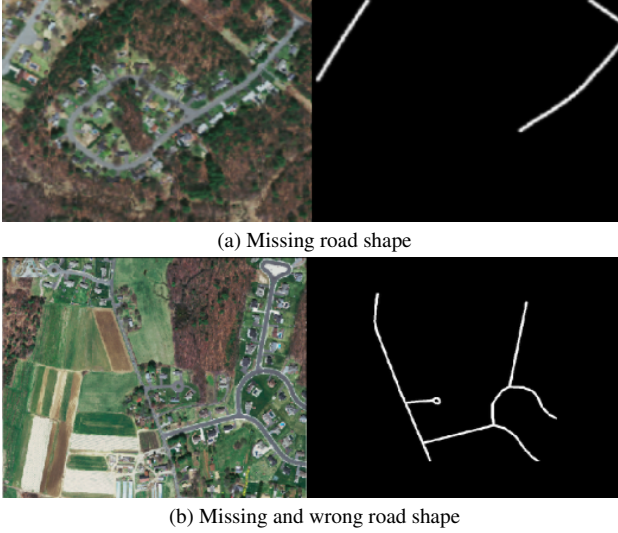


Figure 2. Labeling errors in road map dataset. Figures directly taken from [37]. (a) misses a road segment of the curvy winding road shape in the middle of road map image (b) misses road segments of unstructured winding road shapes on the left and right top area of map and presents the wrong road shapes on the straight roads by missing side roads.

ity from a road-geometric perspective. On the other hand, polynomial curve fitting is adopted to thin the extracted road geometric lines from the road detection system presented by [31]. However, thinning operations are limited when the biased road geometric shapes are extracted. A more thorough survey of custom heuristics can be found at Section 2.6 of [30].

Others further utilize additional information to fix incomplete road maps, such as global navigation satellite system (GNSS) trajectories [50, 52]. For example, common segments of several GPS trajectories can be identified to estimate road centerlines [10, 43] or intersections [12]. However, these approaches are not applicable if trajectory data are not available or sparse on the area of interest. Moreover, applying the extracting algorithms using trajectory data leads to excessive computational resource consumption in handling large areas [52].

### 2.3. Road Geometry Error Localization

In the production setting, one cannot blindly trust the existing road maps due to errors from both human and model predictions. However, relying only on human annotations to detect and fix faulty road maps is often too expensive and has scalability issues [28]. Hence, map companies often employ a semi-automated human-in-the-loop procedure where the model and humans work together [11]. There are many ways to aid human annotation, but our work exclusively concentrates on automatically mending the road

map when the erroneous location is known. In the remaining section, we enumerate the existing methods that identify and localize the faulty road maps so that, when jointly used with our method, one can construct a human-in-the-loop road map fixing system.

Occlusions such as shadows, cars, and buildings that are similar to road features, such as colors, reflectance, and patterns in aerial imagery, are known obstructions for extracting road information [42]. Hence, non-road object detection models, such as neural networks [7, 9, 18, 29], are often employed to avoid manual labeling of bounding boxes [20].

Furthermore, complex road shapes that existing road extraction models often fall short of, such as roundabouts, T-junctions, intersections, or irregular curvy roads, can be prioritized for mending. Road shape detection can also be automated [23], further reducing human labor. HMM (hidden Markov model) based algorithm was also proposed to detect and renew problematic road segments, even though the approach works mainly on rectilinear roads [52].

### 2.4. Image Inpainting

Image inpainting models are used to inpaint (fill in) missing pixels of photographic images to make the completed images look realistic. Context Encoder [40], Globally and Locally Consistent Image Completion (GLCIC) [19], Generative Image inpainting with Contextual Attention [54] and Free-Form Image inpainting with Gated Convolution [53] have shown meaningful achievement in photographic image inpainting problems. However, these models are not optimal for restoring missing pixels of non-photographic images or imagery that presents specific objects, such as road geometry. Generative Image inpainting with Contextual Attention [54] and Free-Form Image inpainting with Gated Convolution [53] are good at filling in parts of photographic images. However, directly applying the aforementioned methods yields limited predictive performance on images of road maps. Hence, we introduce enhancements to the existing approaches to successfully cover road geometries in Section 3.

## 3. Automatically Mending Faulty Road Map Predictions

We introduce a novel data-driven approach for mending faulty road map predictions motivated by the following idea: *Given the abundance of existing images of road maps, why not teach the geometric specifics of roads to a neural network in a self-supervised manner?* Based on this intuition, we leverage the existing image inpainting model and automatically apply modifications to serve the geometric characteristics of road maps. We describe our neural network architecture in Sec. 3.1 and the customized loss in Sec. 3.2.

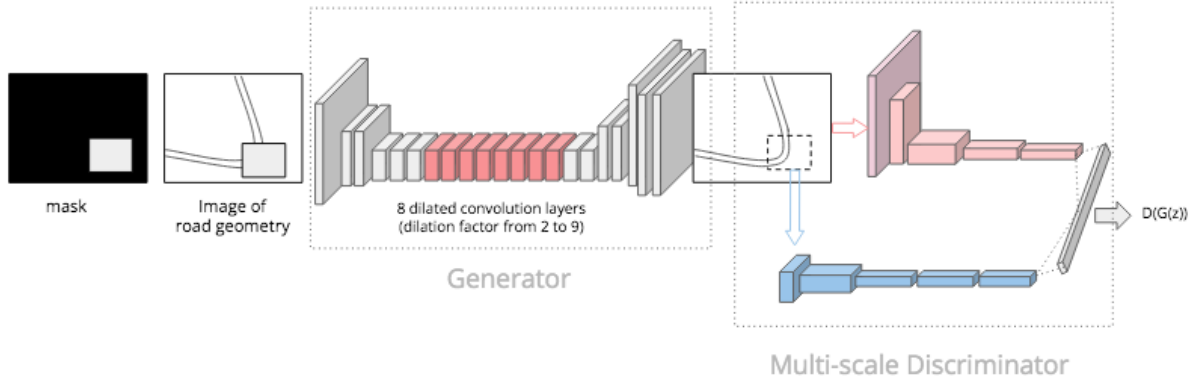


Figure 3. Architecture of our road geometry inpainting model, GLCRC.

### 3.1. Model Architecture

Our model aims to inpaint the geometric road shape in the target area. As mentioned previously in Section 1 and Section 2, we assume that the erroneous location is already localized. We modify the model architecture of GLCIC [19] so that the model can easily handle the latent spatial relationship between the target road segment and the broader range of surrounding around the target road. We denote our model architecture GLCRC (Globally and Locally Consistent Road map Completion). GLCRC consists of two deep neural networks: the generator and the discriminator, shown in Fig. 3.

#### 3.1.1 Generator with Deep Dilated Convolutions

The GLCRC generator has 6 standard convolution layers followed by 8 dilated convolution layers. The 8 dilated convolution layers have an increasing dilation factor that starts from 2 to 9. They enable the model to learn the geometric relationship between the road shape of the inpainted area (*i.e.* target area) and the geometric shape of the road farther away from the area. This is why it is important to keep a high dilation factor in the generator network; to learn the spatial context of the road shape as a whole via the bigger receptive field. Unlike photographic images, which often have the freedom of pixel inaccuracy at a granular level, the inpainted road geometries have to be meticulously correct as actual road shapes in the real map, harmonized with not only neighboring road shapes but also with the overall road geometry in maps. Deconvolution layers are placed after the deep dilated convolutions to generate the inpainted images. Table 1 shows the model architecture of our data-driven road geometry inpainting model.

Type	Filter size	Stride	Dilation	Outputs
conv	$5 \times 5$	$1 \times 1$	-	64
conv	$3 \times 3$	$2 \times 2$	-	128
conv	$3 \times 3$	$1 \times 1$	-	128
conv	$3 \times 3$	$2 \times 2$	-	256
conv	$3 \times 3$	$1 \times 1$	-	256
conv	$3 \times 3$	$1 \times 1$	-	256
dilated conv	$3 \times 3$	$1 \times 1$	2	256
dilated conv	$3 \times 3$	$1 \times 1$	3	256
dilated conv	$3 \times 3$	$1 \times 1$	4	256
dilated conv	$3 \times 3$	$1 \times 1$	5	256
dilated conv	$3 \times 3$	$1 \times 1$	6	256
dilated conv	$3 \times 3$	$1 \times 1$	7	256
dilated conv	$3 \times 3$	$1 \times 1$	8	256
dilated conv	$3 \times 3$	$1 \times 1$	9	256
conv	$3 \times 3$	$1 \times 1$	-	256
conv	$3 \times 3$	$1 \times 1$	-	256
deconv	$4 \times 4$	$1/2 \times 1/2$	-	128
conv	$3 \times 3$	$1 \times 1$	-	128
deconv	$4 \times 4$	$1/2 \times 1/2$	-	64
conv	$3 \times 3$	$1 \times 1$	-	32
output	$3 \times 3$	$1 \times 1$	-	3

Table 1. The generator network architecture of our model, GLCRC.

#### 3.1.2 Multi-scale Context Discriminator

The GLCRC discriminator network follows the multi-scale discriminator architecture [19], which consists of a global and a local context discriminator network. We utilize this architecture to handle the global and local context of the road maps, grasping the overall geometry with its details. The global context discriminator takes  $256 \times 256$  pixel input images and feed-forward to 6 convolution layers. The final fully-connected layer outputs a 1024-dimensional vector. The local context discriminator takes  $128 \times 128$  pixel image patch from an input image, which serves as a target



region to fill in. The output of the local context discriminator is also a 1024-dimensional vector. We concatenate two context vectors to pass through a fully-connected layer and a sigmoid function to represent the probability that a given inpainted image is plausible or not.

### 3.2. Loss function

To achieve better geometric line quality, we adopt loss functions that perform better for Generative Adversarial Networks (GANs) [14].

#### 3.2.1 Avoiding Blurriness via Perceptual Loss

The goal of loss functions is to achieve correctness while increasing the sharpness of the inpainted road geometries. Our generator network is trained with Equation (1), the perceptual loss [21]:

$$\mathcal{L}_P = \frac{1}{W_{i,j}H_{i,j}} \sum_{x=1}^{W_{i,j}} \sum_{y=1}^{H_{i,j}} (\phi_{i,j}(I^O)_{x,y} - \phi_{i,j}(G_{\theta_G}(I^R))_{x,y})^2 \quad (1)$$

where  $\phi_{i,j}$  is the feature map obtained by the  $j$ -th convolution and before the  $i$ -th maxpooling layer within the VGG19 network [24], pretrained on ImageNet [8].  $W_{i,j}$  and  $H_{i,j}$  are the dimensions of the feature maps.  $I^O$  is a original road geometry image and  $I^R$  is input image to be inpainted by model.

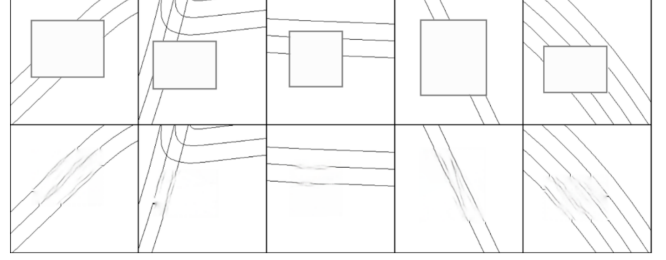
The completion network (*i.e.* generator network) in the original GLCIC [19] use Mean Square Error (MSE) as a loss function. However, we observed that MSE loss is sub-optimal for the road maps compared to the perceptual loss, as it produces more blurry road predictions (Figure 4). Note that the sharpness of the inpainted geometric lines depends on the degree of texture distortion along the road lines. [56] states that perceptual loss captures better textural details and edges versus pixel-wise loss functions such as MSE loss.

#### 3.2.2 Sharper Maps via Relativistic Least Square GAN Loss

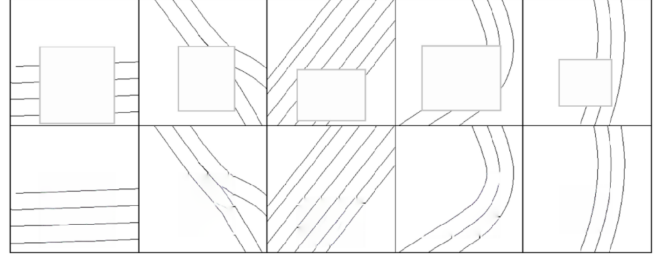
For both global context discriminator and local context discriminator, we adopt Relativistic Least Square GAN (RaLSGAN) loss [22, 25, 34] as a loss function:

$$\mathcal{L}_D^{\text{RaLSGAN}} = \mathbb{E}_{x \sim p_{\text{data}}} [(D(x) - \mathbb{E}_{z \sim p_z} D(G(z)) - 1)^2] + \mathbb{E}_{z \sim p_z} [(D(G(z)) - \mathbb{E}_{x \sim p_{\text{data}}} D(x) + 1)^2]. \quad (2)$$

The vanilla GLCIC model use the Binary Cross Entropy (BCE) loss on discriminator networks. However, empirical findings indicate that RaLSGAN loss helps to generate more textually clean and sharper lines [25], which is a desirable characteristic for road maps.



(a) GLCIC with MSE Loss



(b) GLCIC with Perceptual Loss

Figure 4. Road geometry inpainting results with different losses: (a) MSE loss, and (b) perceptual loss. We mask the road maps (rectangles in the first row) so that the generator can reconstruct the roads within the mask (second row). Blurriness of the roads are notably decreased by utilizing the perceptual loss.

## 4. Experiments

We experimentally demonstrate the effectiveness of our approach by comparing three cases: (1) Vanilla GLCIC, (2) GLCRC (architectural modification only, Section 3.1), and (3) GLCRC with better losses (Section 3.2). We construct the remaining section as follows. Firstly, we describe the dataset (Section 4.1) and the training details (Section 4.2). We finish this section by demonstrating the experimental results (Section 4.3).

### 4.1. Dataset

All the models were trained and evaluated with Massachusetts Road Geometry data [37], which is captured in the state of Massachusetts. The dataset covers over 2600 square kilometers with diverse rural, suburban, and urban areas [1] with a 1m spatial resolution and  $1500 \times 1500$  pixel size, containing 1711 road images.

The grayscale road map images (ground truth images) of the dataset were used for all of our experiments. We divided each image into nine  $500 \times 500$  images, then resized each divided image as an image of  $256 \times 256$  pixels. In all of our experiments, we trained the model with 9972 images and tested the model with 567 images.

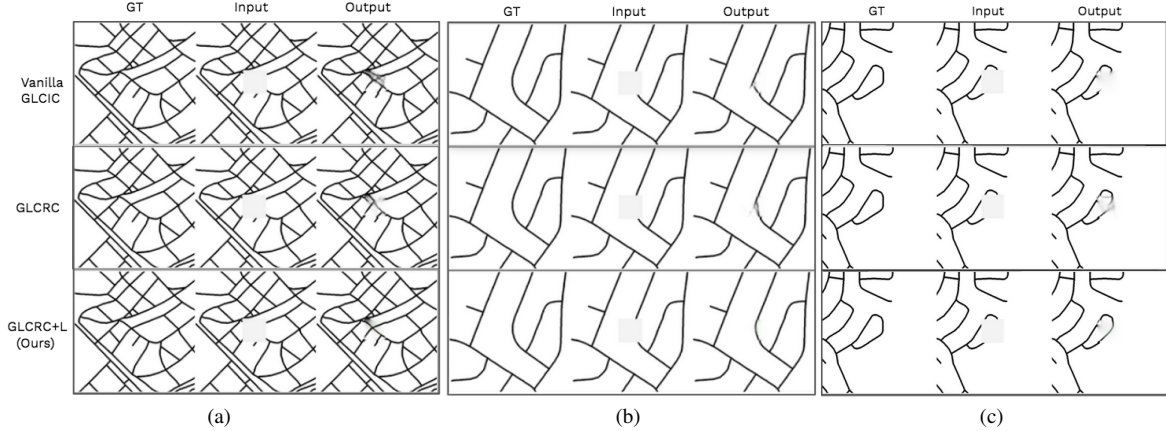


Figure 5. Road inpainting results of Vanilla GLCIC (Baseline), GLCRC (Enhanced Architecture), and GLCRC+L (Ours, GLCRC with perceptual loss and RaLSGAN loss) on various roady types, (a) Intersection (b, c) Curvy road.

Method	Correctness	Completeness	Quality
Vanilla GLCIC	0.787	0.803	0.664
GLCRC	0.789	0.811	0.668
GLCRC+L (Ours)	<b>0.795</b>	<b>0.831</b>	<b>0.671</b>

Table 2. Comparing road map fixing performance. GLCRC denotes architectural modifications to the vanilla GLCIC and GLCRC+L denotes GLCRC with perceptual and RaLSGAN loss.

## 4.2. Training Details

We followed the same training scheme as GLCIC [19]. We pretrained the generator and the discriminator network separately for 90k and 40k steps, respectively. This pre-training approach is often used to train GANs [19] to avoid the instability of adversarial training. After completing the pretraining of each network, the generator and the discriminator are trained in an alternating manner for 90k iterations.

We conducted our experiments with a workstation with 2 NVIDIA GeForce GTX 1080 GPUs. GLCIC and GLCRC training took 36 and 55 hours. With the perceptual and RaLSGAN loss, it took 80 hours. Two factors attributed to the longer training time: (1) the depth of the dilated convolution layers increased, and (2) perceptual loss requires more computation compared to MSE loss. However, inference took approximately 1 second per each image regardless of the model.

## 4.3. Experimental Results

We conduct quantitative (Table 2) and qualitative analysis (Figure 1) on whether the modifications are effective. Further, we also evaluate separately with respect to various road types (Table 3) to verify to check the method’s robustness on each. We choose three random road maps per each road type. These road types, such as Intersection, T-

junction, and Curvy road, are particularly challenging to be restored by trajectory data-based post-processing methods.

We use three metrics, Correctness, Completeness, and Quality, which are widely accepted in road extraction tasks [6, 48, 49]:

$$\text{Correctness} = \frac{TP}{TP + FN}$$

$$\text{Completeness} = \frac{TP}{TP + FP}$$

$$\text{Quality} = \frac{TP}{TP + FN + FP}$$

where TP is True Positive, FN is False Negative, and FP is False Positive.

Table 2 demonstrates the performance impact on various modifications: GLCRC being the architectural and GLCRC+L being the training loss modifications. We can clearly observe that our approach shows the best image quality in the road geometry inpainting problem. Furthermore, Figure 1 shows the effectiveness of our method on various road types, implying that it understands underlying road geometries to reconstruct the road location.

We also compare and evaluate the modifications on separate road types qualitatively (Figure 5) and quantitatively (Table 3). Figure 5 demonstrates that complex road shapes such as multiple T-junction areas and irregular curvy roads are successfully handled via our method. Even though architectural changes can improve the overall road shapes, one has to employ perceptual loss and RaLSGAN loss to enhance the smoothness and the sharpness of roads. Further, Table 3 indicates that ours shows superior performance in all the complex road types and evaluation metrics.

Road type	Method	Correctness	Completeness	Quality
Straight road	Vanilla GLCIC	0.787	0.786	0.649
	GLCRC	0.750	0.806	0.635
	GLCRC+L (Ours)	<b>0.894</b>	<b>0.898</b>	<b>0.811</b>
Curvy road	Vanilla GLCIC	0.762	0.757	<b>0.613</b>
	GLCRC	0.723	0.789	0.606
	GLCRC+L (Ours)	<b>0.754</b>	<b>0.766</b>	<b>0.613</b>
T-junction	Vanilla GLCIC	0.775	0.788	0.642
	GLCRC	0.785	0.792	0.651
	GLCRC+L (Ours)	<b>0.842</b>	<b>0.849</b>	<b>0.733</b>
Intersection	Vanilla GLCIC	0.775	0.788	0.642
	GLCRC	0.785	0.792	0.651
	GLCRC+L (Ours)	<b>0.786</b>	<b>0.793</b>	<b>0.652</b>

Table 3. Comparing road map fixing performance on various road geometries. GLCRC denotes architectural modifications to the vanilla GLCIC and GLCRC+L denotes GLCRC with perceptual and RaLSGAN loss.

## 5. Conclusion

Even though numerous advances have been made to the automated extraction of road maps from satellite imagery fueled by the abundance and availability of data, many still rely on hand-crafted heuristics and algorithms to fix faulty road map predictions. Our work shed new light on the road-mending techniques motivated by the data-driven machine learning algorithms that prevail in vision applications today. We introduce a novel method based on the image inpainting technique by regarding faulty (noisy, missing, or wrong) road map predictions as the image to inpaint. We modify the existing image inpainting approaches to handle the geometric context while maintaining accuracy and crispness for road maps. Our method does not require specific tuning on the numerous real-world road types nor additional trajectory data to interpolate; it only needs a sufficient amount of data to enhance the predictions. Experiments demonstrate that our method is robust to various real-world road geometries.

## References

- [1] Abolfazl Abdollahi, Biswajeet Pradhan, Nagesh Shukla, Subrata Chakraborty, and Abdullah Alamri. Deep learning approaches applied to remote sensing datasets for road extraction: A state-of-the-art review. *Remote Sensing*, 12:1444, 05 2020. **2, 5**
- [2] Sultan Alamri. Independent map enhancement for a spatial road network: Fundamental applications and opportunities. *ISPRS International Journal of Geo-Information*, 10(1), 2021. **2**
- [3] Ruzena Bajcsy and Mohamad Tavakoli. Computer recognition of roads from satellite pictures. *IEEE Transactions on Systems, Man, and Cybernetics*, 6:623–637, 1976. **2**
- [4] Favyen Bastani, Songtao He, Sofiane Abbar, Mohammad Alizadeh, Hari Balakrishnan, Sanjay Chawla, Sam Madden, and David DeWitt. Roadtracer: Automatic extraction of road networks from aerial images. In *Proceedings of the IEEE Conference on Computer Vision and Pattern Recognition*, pages 4720–4728, 2018. **1, 2**
- [5] Favyen Bastani and Samuel Madden. Beyond road extraction: A dataset for map update using aerial images. In *Proceedings of the IEEE/CVF International Conference on Computer Vision*, pages 11905–11914, 2021. **1**
- [6] Aleksey Boyko and Thomas Funkhouser. Extracting roads from dense point clouds in large scale urban environment. *Isprs Journal of Photogrammetry and Remote Sensing - ISPRS J PHOTOGRAMM*, 66, 12 2011. **6**
- [7] Fei Deng, Junhua Kang, Li Penglong, and Fang Wan. Automatic true orthophoto generation based on three-dimensional building model using multiview urban aerial images. *Journal of Applied Remote Sensing*, 9:095087, 03 2015. **3**
- [8] Jia Deng, Wei Dong, Richard Socher, Li-Jia Li, Kai Li, and Li Fei-Fei. Imagenet: A large-scale hierarchical image database. In *2009 IEEE conference on computer vision and pattern recognition*, pages 248–255. Ieee, 2009. **5**
- [9] Jian Ding, Nan Xue, Gui-Song Xia, Xiang Bai, Wen Yang, Michael Ying Yang, Serge Belongie, Jiebo Luo, Mihai Datcu, Marcello Pelillo, et al. Object detection in aerial images: A large-scale benchmark and challenges. *IEEE transactions on pattern analysis and machine intelligence*, 44(11):7778–7796, 2021. **3**
- [10] Stefan Edelkamp and Stefan Schrödl. Route planning and map inference with global positioning traces. In *Computer science in perspective*, pages 128–151. Springer, 2003. **3**
- [11] Ankit Laddha et al. Map-supervised road detection. In *IEEE Intelligent Vehicles Symposium*. IEEE, 2016. **3**
- [12] Alireza Fathi and John Krumm. Detecting road intersections from gps traces. In *International conference on geographic information science*, pages 56–69. Springer, 2010. **3**

- [13] Alberto Garcia-Garcia, Sergio Orts-Escolano, Sergiu Oprea, Victor Villena-Martinez, and Jose Garcia-Rodriguez. A review on deep learning techniques applied to semantic segmentation. *arXiv preprint arXiv:1704.06857*, 2017. 1
- [14] Ian Goodfellow, Jean Pouget-Abadie, Mehdi Mirza, Bing Xu, David Warde-Farley, Sherjil Ozair, Aaron Courville, and Yoshua Bengio. Generative adversarial nets. In *Advances in neural information processing systems*, pages 2672–2680, 2014. 5
- [15] Zhen He, Tao Wu, Zhipeng Xiao, and Hangen He. Robust road detection from a single image using road shape prior. In *2013 IEEE International Conference on Image Processing*, pages 2757–2761, 2013. 2
- [16] Aaron Holmes. Apple told congress it has spent 'billions of dollars' on apple maps. *Business Insider*, 2019. 1
- [17] Leslie Hook. Uber to pour \$500m into global mapping project. *Financial Times*, 2016. 1
- [18] X Hu and X Li. Fast occlusion and shadow detection for high resolution remote sensing image combined with lidar point cloud. *ISPRS-International Archives of the Photogrammetry, Remote Sensing and Spatial Information Sciences*, 39:399–402, 2012. 3
- [19] Satoshi Iizuka, Edgar Simo-Serra, and Hiroshi Ishikawa. Globally and locally consistent image completion. *ACM Trans. Graph.*, 36(4):107:1–107:14, 2017. 2, 3, 4, 5, 6
- [20] Fahmida Islam, M M Nabi, and John E. Ball. Off-road detection analysis for autonomous ground vehicles: A review. *Sensors*, 22(21), 2022. 3
- [21] J. Johnson, A. Alahi, , and L. Fei-Fei. Perceptual losses for real-time style transfer and super-resolution. In *European Conference on Computer Vision*, 2016. 5
- [22] Alexia Jolicoeur-Martineau. The relativistic discriminator: a key element missing from standard gan. *arXiv preprint arXiv:1807.00734*, 2018. 5
- [23] Mohamad Haniff Junos, Anis Salwa Mohd Khairuddin, and Mahidzal Dahari. Automated object detection on aerial images for limited capacity embedded device using a lightweight cnn model. *Alexandria Engineering Journal*, 61(8):6023–6041, 2022. 3
- [24] Orest Kupyn, Volodymyr Budzan, Mykola Mykhailych, Dmytro Mishkin, and Jiří Matas. Deblurgan: Blind motion deblurring using conditional adversarial networks. In *Proceedings of the IEEE conference on computer vision and pattern recognition*, pages 8183–8192, 2018. 5
- [25] Orest Kupyn, Tetiana Martyniuk, Junru Wu, and Zhangyang Wang. Deblurgan-v2: Deblurring (orders-of-magnitude) faster and better. In *Proceedings of the IEEE/CVF International Conference on Computer Vision*, pages 8878–8887, 2019. 5
- [26] Y. Lecun, L. Bottou, Y. Bengio, and P. Haffner. Gradient-based learning applied to document recognition. *Proceedings of the IEEE*, 86(11):2278–2324, 1998. 2
- [27] Jun Li, Qiming Qin, Jiawei Han, Lu-An Tang, and Kin Hou Lei. Mining trajectory data and geotagged data in social media for road map inference. *Transactions in GIS*, 19(1):1–18, 2015. 1
- [28] Justin Liang, Namdar Homayounfar, Wei-Chiu Ma, Shenlong Wang, and Raquel Urtasun. Convolutional recurrent network for road boundary extraction. In *Proceedings of the IEEE/CVF Conference on Computer Vision and Pattern Recognition*, pages 9512–9521, 2019. 2, 3
- [29] Wentong Liao, Xiang Chen, Jingfeng Yang, Stefan Roth, Michael Goesele, Michael Ying Yang, and Bodo Rosenhahn. Lr-cnn: Local-aware region cnn for vehicle detection in aerial imagery. *arXiv preprint arXiv:2005.14264*, 2020. 3
- [30] Pengfei Liu, Qing Wang, Gaochao Yang, Lu Li, and Huan Zhang. Survey of road extraction methods in remote sensing images based on deep learning. *PFG-Journal of Photogrammetry, Remote Sensing and Geoinformation Science*, 90(2):135–159, 2022. 1, 2, 3
- [31] Ruyi Liu, Qiguang Miao, Jianfeng Song, Yi-Ning Quan, Yunnan Li, Pengfei Xu, and Jing Dai. Multiscale road centerlines extraction from high-resolution aerial imagery. *Neurocomputing*, 329:384–396, 2019. 2, 3
- [32] Jonathan Long, Evan Shelhamer, and Trevor Darrell. Fully convolutional networks for semantic segmentation. In *Proceedings of the IEEE conference on computer vision and pattern recognition*, pages 3431–3440, 2015. 2
- [33] Prajowal Manandhar, Prashanth Reddy Marpu, Zeyar Aung, and Farid Melgani. Towards automatic extraction and updating of vgi-based road networks using deep learning. *Remote Sensing*, 11(9):1012, 2019. 2
- [34] Xudong Mao, Qing Li, Haoran Xie, Raymond YK Lau, Zhen Wang, and Stephen Paul Smolley. Least squares generative adversarial networks. In *Proceedings of the IEEE international conference on computer vision*, pages 2794–2802, 2017. 5
- [35] Gellért Mátyus, Wenjie Luo, and Raquel Urtasun. Deep-roadmapper: Extracting road topology from aerial images. In *Proceedings of the IEEE international conference on computer vision*, pages 3438–3446, 2017. 1
- [36] Greg Miller. The huge, unseen operation behind the accuracy of google maps. *Wired*, 2014. 1
- [37] Volodymyr Mnih. *Machine Learning for Aerial Image Labeling*. PhD thesis, University of Toronto, 2013. 3, 5
- [38] Volodymyr Mnih and Geoffrey E Hinton. Learning to detect roads in high-resolution aerial images. In *European conference on computer vision*, pages 210–223. Springer, 2010. 2
- [39] OpenStreetMap contributors. Planet dump retrieved from <https://planet.osm.org>. <https://www.openstreetmap.org>, 2017. 2
- [40] Deepak Pathak, Philipp Krahenbuhl, Jeff Donahue, Trevor Darrell, and Alexei A. Efros. Context encoders: Feature learning by inpainting. In *Proceedings of International Conference on Computer Vision and Pattern Recognition*, 2016. 2, 3
- [41] Hamid Reza Riyahi Bakhtyari, Abolfazl Abdollahi, and Hani Rezayan. Semi automatic road extraction from digital images. *The Egyptian Journal of Remote Sensing and Space Science*, 20, 03 2017. 2
- [42] Shunta Saito, Takayoshi Yamashita, and Yoshimitsu Aoki. Multiple object extraction from aerial imagery with convolutional neural networks. *Electronic Imaging*, 2016:1–9, 02 2016. 3



- [43] Stefan Schroedl, Kiri Wagstaff, Seth Rogers, Pat Langley, and Christopher Wilson. Mining gps traces for map refinement. *Data mining and knowledge Discovery*, 9(1):59–87, 2004. 3
- [44] Qian Shi, Xiaoping Liu, and Xia Li. Road detection from remote sensing images by generative adversarial networks. *IEEE access*, 6:25486–25494, 2017. 2
- [45] pankaj Singh and Rahul Garg. Automatic road extraction from high resolution satellite image using adaptive global thresholding and morphological operations. *Journal of the Indian Society of Remote Sensing*, 41, 10 2012. 2
- [46] Chinnathevar Sujatha and Dharmar Selvathi. Connected component-based technique for automatic extraction of road centerline in high resolution satellite images. *EURASIP Journal on Image and Video Processing*, 2015, 12 2015. 2
- [47] Yiting Tao, Miaozhong Xu, Fan Zhang, Bo Du, and Liangpei Zhang. Unsupervised-restricted deconvolutional neural network for very high resolution remote-sensing image classification. *IEEE Transactions on Geoscience and Remote Sensing*, 55(12):6805–6823, 2017. 2
- [48] Jianhua Wang, Qimin Qin, Zhongling Gao, Jianghua Zhao, and Xin Ye. A new approach to urban road extraction using high-resolution aerial image. *ISPRS International Journal of Geo-Information*, 5:114, 07 2016. 2, 6
- [49] Christian Wiedemann, Christian Heipke, Helmut Mayer, and Olivier Jamet. Empirical evaluation of automatically extracted road axes. *Empirical evaluation techniques in computer vision*, 12:172–187, 1998. 6
- [50] Hangbin Wu, Zeran Xu, and Guangjun Wu. A novel method of missing road generation in city blocks based on big mobile navigation trajectory data. *ISPRS International Journal of Geo-Information*, 8(3), 2019. 3
- [51] Songbing Wu, Chun Du, Hao Chen, Yingxiao Xu, Ning Guo, and Ning Jing. Road extraction from very high resolution images using weakly labeled openstreetmap centerline. *ISPRS International Journal of Geo-Information*, 8(11):478, 2019. 2
- [52] Tao Wu, Longgang Xiang, and Jianya Gong. Updating road networks by local renewal from gps trajectories. *ISPRS International Journal of Geo-Information*, 5(9), 2016. 3
- [53] Jiahui Yu, Zhe Lin, Jimei Yang, Xiaohui Shen, Xin Lu, and Thomas Huang. Free-form image inpainting with gated convolution. In *Proceedings of International Conference on Computer Vision (ICCV)*, 2019. 2, 3
- [54] Jiahui Yu, Zhe Lin, Jimei Yang, Xiaohui Shen, Xin Lu, and Thomas S. Huang. Generative image inpainting with contextual attention. In *Proceedings of Computer Vision and Pattern Recognition (CVPR)*, 2018. 2, 3
- [55] Jing Zhang, Lu Chen, Chao Wang, Li Zhuo, Qi Tian, and Xi Liang. Road recognition from remote sensing imagery using incremental learning. *IEEE Transactions on Intelligent Transportation Systems*, 18(11):2993–3005, 2017. 1
- [56] Kuan Zhang, Haoji Hu, Kenneth Philbrick, Gian Marco Conte, Joseph D Sobek, Pouria Rouzrokh, and Bradley J Erickson. Soup-gan: Super-resolution mri using generative adversarial networks. *Tomography*, 8(2):905–919, 2022. 5
- [57] Ling Zheng, Bijun Li, Bo Yang, Huashan Song, and Zhi Lu. Lane-level road network generation techniques for lane-level maps of autonomous vehicles: A survey. *Sustainability*, 11(16):4511, 2019. 2